Research Article

High-Performance Graphene Oxide/Polypyrrole/*Ziziphus jujuba*/*Prunus dulcis* Ternary Composite Electrodes for Supercapacitor for Sensor Applications

Senthil Kumar Kandasamy ,[1] **S. Maheswaran** ,[1] **K. R. Kavitha** ,[2] **D. Karthikeyan**,[3] **J. Indra**,[4] **K. Sheikdavood** ,[5] **Y. Syamala**,[6] **K. Srilakshmi**,[7] **Chandrasekaran Arumugam** ,[1] and **Dhivya Balamoorthy** [8]

[1]*Department of Electronics and Communication Engineering, Kongu Engineering College, 638060, Tamil Nadu, India*
[2]*Department of Electronics and Communication Engineering, Sona College of Technology, 636005, Salem, Tamil Nadu, India*
[3]*Department of Electronics and Communication Engineering, Kongunadu College of Engineering and Technology, 621215, Trichy, Tamil Nadu, India*
[4]*Department of Electronics and Communication Engineering, KPR Institute of Engineering and Technology, 641407, Coimbatore, Tamil Nadu, India*
[5]*Department of Electronics and Communication Engineering, M.Kumarasamy College of Engineering, 639113, Karur, Tamil Nadu, India*
[6]*Department of IoT, Seshadri Rao Gudlavalleru Engineering College, JNTUK, Kakinada, Andhra Pradesh, India*
[7]*Department of Electronics and Communication Engineering, Seshadri Rao Gudlavalleru Engineering College, JNTUK, Kakinada, Andhra Pradesh, India*
[8]*Department of Hydraulic and Water Resource Engineering, Wollega University, Nekemte, Ethiopia*

Correspondence should be addressed to S. Maheswaran; mmaheswaraneie@gmail.com
and Dhivya Balamoorthy; dhivyabalamoorthy@wollegauniversity.edu.et

Supercapacitor electrodes synthesized from activated carbon (AC) has high energy and power capabilities as they have larger surface area, greater conductivity, and also AC has the ability to optimize the properties of supercapacitors. Supercapacitor has gained its attention due to its fast charging/discharging speed and long-term stability than the normal batteries. In this work, GO/PPy/AC composite electrodes was synthesized to increase the specific capacitance and the energy storage capability of supercapacitor through modified hummers' method, sacrificial template polymerization method, and hydrothermal method. Here, the AC was derived from seeds of *Ziziphus jujuba* and shells of *Prunus dulcis*. The performances of GO, GO/PPy, GO/PPy/ACZJ, and GO/PPy/ACPD electrodes were evaluated using 6 M KOH electrolyte at different current densities and scan rates. The electrochemical properties of the electrodes were characterized by CV, GCD, and EIS analysis to study the suitability of the electrode material. GO/PPy/ACPD electrode exhibited the specific capacitance of 1217.1, 456.67, 270.44, and 90.88 $F\,g^{-1}$ with current densities of 1, 2, 4, and 10 $A\,g^{-1}$, respectively. GO/PPy/ACPD has high specific capacitance of 1217.1 $F\,g^{-1}$ at 1 $A\,g^{-1}$. The enhanced electrochemical performance is due to better surface area and higher specific capacitance.

1. Introduction

In outlook, energy is the major concern for all the works. Simultaneously, energy demand and depletion are the seri-ous factors. To minimize the environmental effects and the cost constraints, the waste obtained from green products may provide a substitute to the electrode material. To reach the quickly increasing worldwide demand of energy

without destroying the environment, it is significant to lessen dependence of fossil fuel sources. Activated carbon can be prepared from any agricultural waste. In this regard, to support the renewable energy, the uses of energy storage devices are inevitable. Among the energy storage devices such as battery, capacitor, and supercapacitor, supercapacitor holds a great position. So researchers are producing electrode materials for supercapacitor. So several types of electrode materials were synthesized and tested for energy storage in terms of power density, energy density, and specific capacitance. EDLC, pseudocapacitor, and hybrid are the classification of supercapacitor. Here, EDLC can be achieved through the carbonaceous materials and pseudocapacitors achieved through conducting polymers and metal oxides [1]. Hybrid is done through composite materials based symmetric or combination of carbonaceous electrode in one side and conducting polymer electrodes in another side [1]. Application of the supercapacitor includes in the range of high power devices to low power devices.

From the carbonaceous materials, graphene oxide (GO) is mainly considered for its conductivity, and also it acted as a substrate for the better growth of conducting polymer [1]. Similarly, activated carbon developed from biomaterial is having a considerable effect [2, 3]. Microwave-treated graphene is also considered as candidate for electrochemical devices because of its porous nature [4]. Conducting polymer polyaniline [5] is one of the materials used in supercapacitors. Currently, researchers are working on the electrode materials for supercapacitor using composites such as graphene/metal oxide composite [6] and graphene/conducting polymer composite [7–10]. Guo Y. et al. [11] produced porous carbon from almond shell with the surface area of $3249.68 \, m^2 \, g^{-1}$. Pseudocapacitance and wettability can be achieved from the presence of heteroatoms and micropores used to reduce the thickness of EDLC. Li et al. [12] prepared *jujube*-derived carbon with hierarchical porous structure and abundant heteroatom groups. Through one-pot approach, Sun et al. [13] prepared permeable carbon with rich oxygen-containing groups and interconnected meso-, micro-, and macropores. The porous carbon obtained from *jujube* fruits exhibited more than 90% of capacitance even after 130000 cycles and also displayed $324 \, F \, g^{-1}$ at $100 \, A \, g^{-1}$ in $6 \, M$ KOH [14]. Theophil et al. synthesized ZnO nanoparticles from almond shell and used it for supercapacitor [15]. Jiménez et al. [16] synthesized microporous carbon materials from grape seeds through cyclic oxidation. By nondestructive activation of sawdust, reduction of defects and improvements of surface area and conductivity can be achieved [17] using KOH.

Activated carbon is obtained from *Syzygium cumini* and *Chrysopogon zizanioides* by physical activation with excellent rate capability [18]. Mesoporous volume can be increased because of the presence of silica before the activation [19]. Similarly, by hydrothermal method, Jeniffer and Vimala [20] prepared activated carbon from *Eucalyptus globulus* seed with $150 \, F \, g^{-1}$. Composite made up of rGO and $NiCo_2S_4$ through microwave method exhibited $1320 \, F \, g^{-1}$ [21]. To avoid the problems such as toxicity and harmful nature associated with the reducing agent, green tea polyphenols were used, and also the composite exhibited good electrochemical performance for covalent bond [22]. With respect to
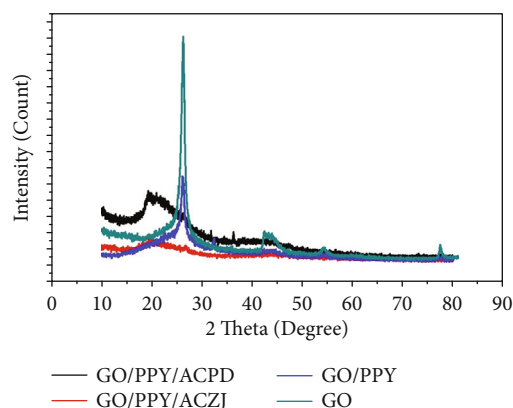

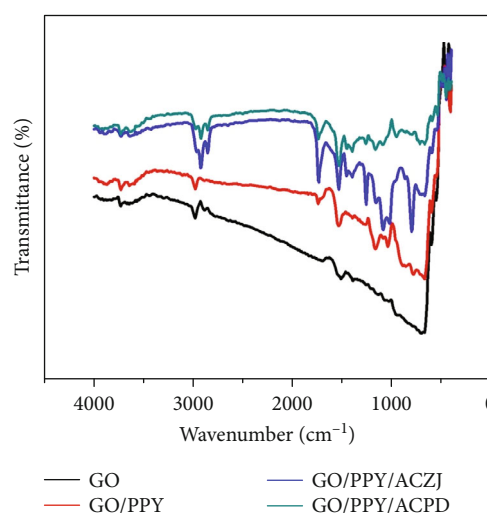FIGURE 1: XRD pattern of as prepared samples.

FIGURE 2: FTIR spectra of as prepared samples.

the electrochemical impedance spectroscopy analysis, the charge transfer resistance of conducting polyaniline can be minimized with the help of azobenzene units [23]. The ternary composite exhibited higher specific capacitance [9]. Using an in situ polymerization, Wang et al. [24] synthesized graphene oxide/PANI composite electrode with $531 \, F \, g^{-1}$ specific capacitance. Similarly, use chronoamperometry PANI/GO which has been coated on stainless steel [25] with a specific capacitance of $1140 \, F \, g^{-1}$. PANI has been crafted on RGO using chemical oxidative polymerization with a specific capacitance of $250 \, F \, g^{-1}$ [26]. Senthil Kumar et al. [27] synthesized activated carbon from biomass wastes such as banana peels, orange peels, and potato starch.

Vinay et al. [28] used agricultural waste to extract porous nanocarbon for supercapacitors with $174 \, F \, g^{-1}$ at $0.1 \, A \, g^{-1}$ in $4.0 \, M$ KOH. Bhimanaboina et al. [29] used waste tissue papers with highly porous Mn_3O_4 hollow microtubes for pseudocapacitor applications to increase the porosity. Yuhao et al. [30] used longan shell as a precursor and synthesized 3D carbon with copious consistent pores and reasonable heteroatoms by means of carbonization and activation to obtain specific capacitance $359 \, F \, g^{-1}$. Yan Lei and Zhi Shu [31] obtained carbon through *Salvia*
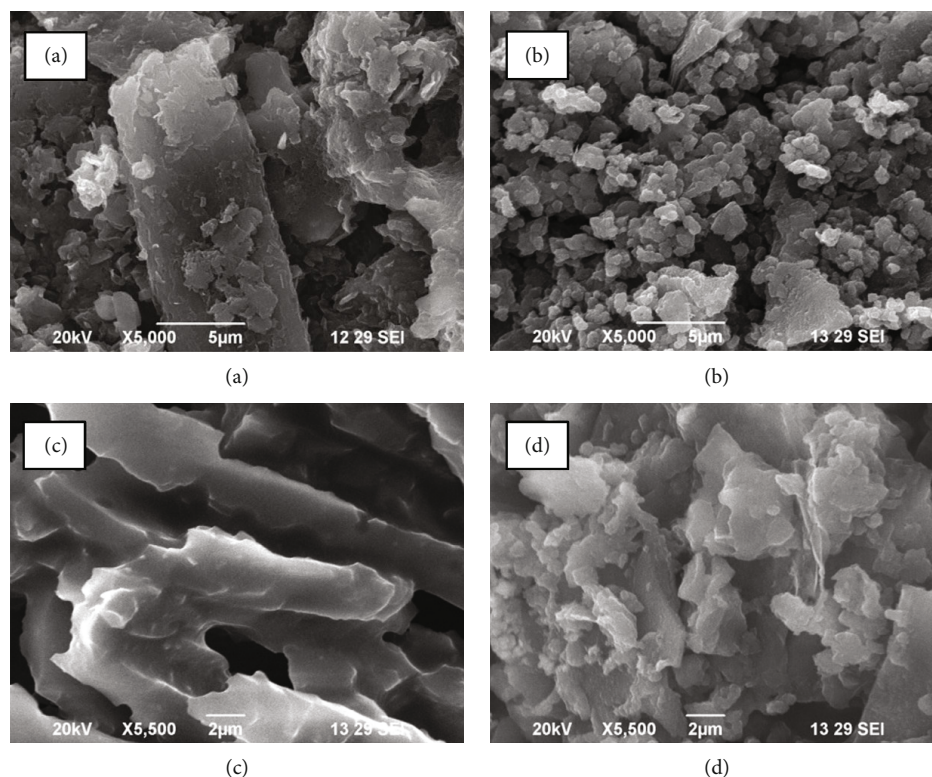
FIGURE 3: SEM images of GO, GO/PPy, GO/PPy/ACZJ, and GO/PPy/ACPD composite.

miltiorrhiza with specific surface area (SSA) of 1715.3 $m^2 g^{-1}$. Sofia and Vimala [32] prepared activated carbon (AC) from *Eucalyptus globulus* seed by a simple hydrothermal method followed by chemical activation. Kenny et al. [33] extracted waste from jackfruit and durian to make carbon aerogel and nitrogen doping with increased surface area and specific capacitance.

Dawei et al. [34] used walnut shell for the preparation of AC with KOH activation to increase the specific surface area. Le et al. [35] used *Areca* palm leaves to derive porous carbon as the electrode using a fast carbonization method followed by in situ chemical activation. Murugan et al. [36] used *Syzygium cumini* and *Chrysopogon zizanioides* to extract porous activated carbon for high-energy density symmetric super capacitors using carbonization and CO_2 activation. Karnan et al. [37] used *Thespesia populnea* to derive AC for supercapacitor. Khodary et al. [38] prepared PPy adorned MnO_2/rGO with 295.83 $F g^{-1}$. Supercapacitor electrodes developed from GO/metal oxide [39], GO/PANI [40], were having high specific capacitance. Activated carbon can be obtained from various sources with high carbon content; Acacia leucophloea wood sawdust [41], black liquor [42], and cotton yarn were also used [43].

In this work, activated carbon was separately obtained from activation of *Jujube seeds* and *Prunus dulcis* shell. Graphene oxide was obtained from modified hummers' method. GO/PPY composite was obtained through sacrificial template polymerization [44]. Finally, ternary composite made up of activated carbon, GO, and PPy was obtained through hydrothermal method[27]. Then all the

as-prepared samples were electrochemically analyzed to understand the electrochemical properties of the electrodes. The electrochemical analyses were performed at an OrigaLys electrochemical workstation using 6 M KOH. The three-electrode system comprises the working electrode, a platinum counter electrode, and an Ag/AgCl reference electrode.

2. Experimental Section

2.1. Materials Used. Graphite, polypyrrole, potassium permanganate, potassium persulfate, sodium nitrate, hydrogen peroxide, concentrated H_2SO_4, and ethanol were purchased. *Jujube seeds* and *Prunus dulcis* shells were obtained from the local factory located at erode.

2.2. Synthesis of GO. Graphene oxide was produced from graphite by modified hummers method by slowly adding 16 g of graphite in a beaker containing 184 ml of conc. H_2SO_4. After 10 minutes, 9 g of $NaNO_3$ was added. After constant magnetic stirring for an hour, 12 g of $KMnO_4$ was further added. Then it was stirred for 14 hours at 10° C, and the concentration was reduced by adding 168 ml of distilled water. After 1 hour, 33 ml of H_2O_2 is mixed and stirred for 1 hour. Finally, it was filtered using Whatman paper. The residue was taken alone and washed by ethanol and distilled water for 3 times. Then it was kept in an oven at 90° C for 1 day. Finally, powdered form of graphene oxide was obtained.
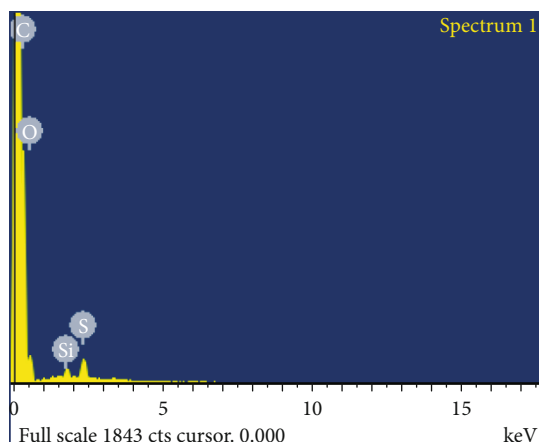
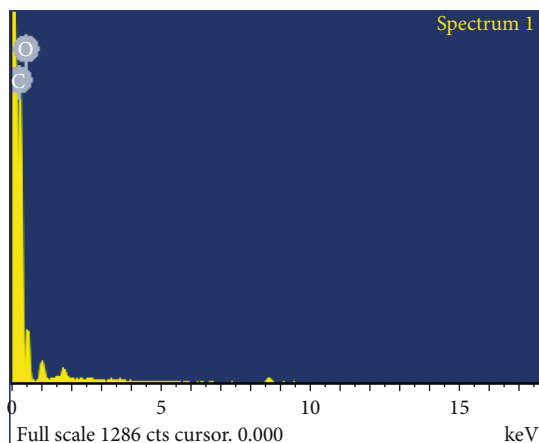| Element	App Conc.	Intensity Corrn.	Weight%	Weight% Sigma	Atomic%
C K	18.68	0.9861	60.97	1.72	68.38
O K	5.07	0.4539	35.95	1.69	30.26
Si K	0.29	0.9298	1.01	0.18	0.49
S K	0.62	0.9581	2.07	0.24	0.87
Totals			100.00		

(a)
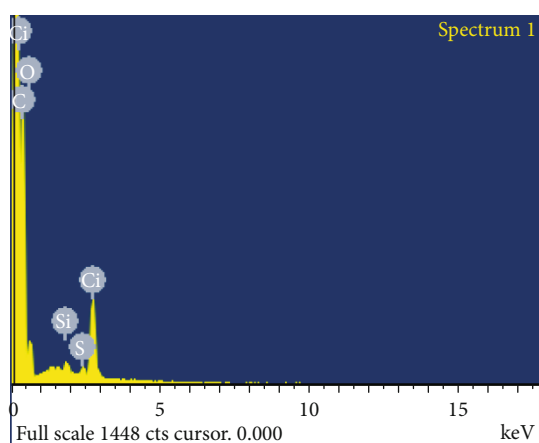
Element	App Conc.	Intensity Corrn.	Weight%	Weight% Sigma	Atomic%
C K	21.93	0.7444	71.73	1.56	79.24
O K	3.32	0.3631	22.23	1.52	18.43
Si K	0.19	0.9651	0.49	0.12	0.23
S K	0.20	0.9881	0.49	0.13	0.20
Cl K	1.74	0.9351	5.06	0.30	1.89
Totals			100.00		

(b)

Element	App Conc.	Intensity Corrn.	Weight%	Weight% Sigma	Atomic%
C K	21.22	1.3566	61.43	1.50	67.96
O K	4.61	0.4679	38.57	1.50	32.04
Totals			100.00		

(c)

FIGURE 4: EDX spectra of GO, GO/PPy, GO/PPy/ACZJ, and GO/PPy/ACPD composite.

2.3. Preparation of Activated Carbon. Activated carbon was obtained from *Ziziphus jujuba* seed and *Prunus dulcis* shell using carbonization and chemical activation process. Initially, they were kept in muffle furnace separately at 450° C for 6 hours [41]. The carbonized form of *Ziziphus jujuba* seed and *Prunus dulcis* was obtained. The activator used was KOH/H_2SO_4 to increase the pores in activated carbon for more absorption of ions in electrolyte. They were mixed and kept in muffle furnace at appropriate temperature and time. The activated carbon (AC) was washed and filtered using filter. It was then dried using an oven to remove the wetness in the substance for a day at 80° C, and powered activated carbon was obtained using pestle mortar.
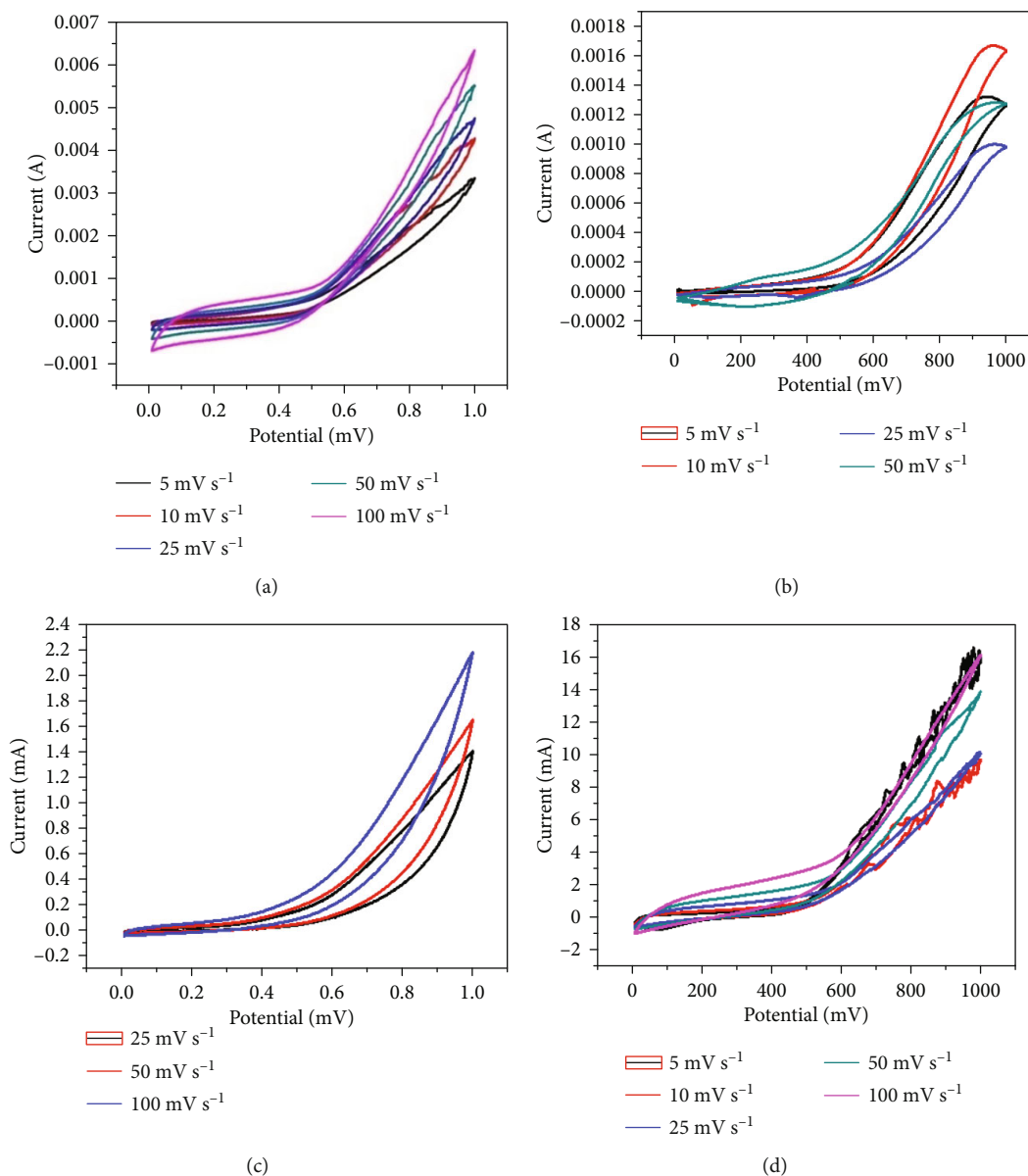
(a)

(b)

(c)

(d)

FIGURE 5: CV curves of (a) GO, (b) GO/PPY, (c) GO/PPy/ACZJ, and (d) GO/PPy/ACPD.

2.4. Synthesis of GO/PPy Composite. GO/PPy composite was made by sacrificial template polymerization method. Initially, 1 g of GO/MnO$_2$ and 60 ml of distilled water were added and stirred for 10 m at 500 rpm. Here MnO$_2$ nanoslices were used as template for deposition of polypyrrole. 12 ml of concentrated HCl and 12 ml of pyrrole monomer were added and stirred for 60 m at 800 rpm using magnetic stirrer. Then it was filtered using Whatman filter paper and kept in oven for 6 hours at 80° C. Thus the graphene oxide/polypyrrole composite was obtained.

2.5. Preparation of GO/PPy/ACPD and GO/PPy/ACZJ Composite. All the ternary composites were prepared by hydrothermal method. It is a solution reaction-based approach. The preparation procedure of the composite is as follows. GO/PPy/AC composite was prepared using hydro-

thermal process. Initially, 0.1 g of GO/PPy and 1 g of activated carbon from *Ziziphus jujuba* (ACZJ) seed was weighed. Then it was kept in the autoclave, and 100 ml of distilled water was added. 150° C was maintained at 250 rpm for 180 minutes. Then it was allowed to cool for few minutes. The mixture was continually washed using ethanol and DD water and then filtered using Whatman filter paper and kept in an oven to remove wetness at 85° C for 24 hours. Thus the GO/PPy/ACZJ composite was obtained. The same hydrothermal process was repeated using 0.1 g of GO/PPy and 1 g of activated carbon from *Prunus dulcis* shell (ACPD), 100 ml of distilled water at 150° C maintained at 250 rpm for 180 minutes. Thus the GO/PPy/ACPD composite was obtained.

2.6. Structural and Electrochemical Measurements. All the samples were structurally analyzed using XRD. All the

(a)

(b)

(c)

(d)
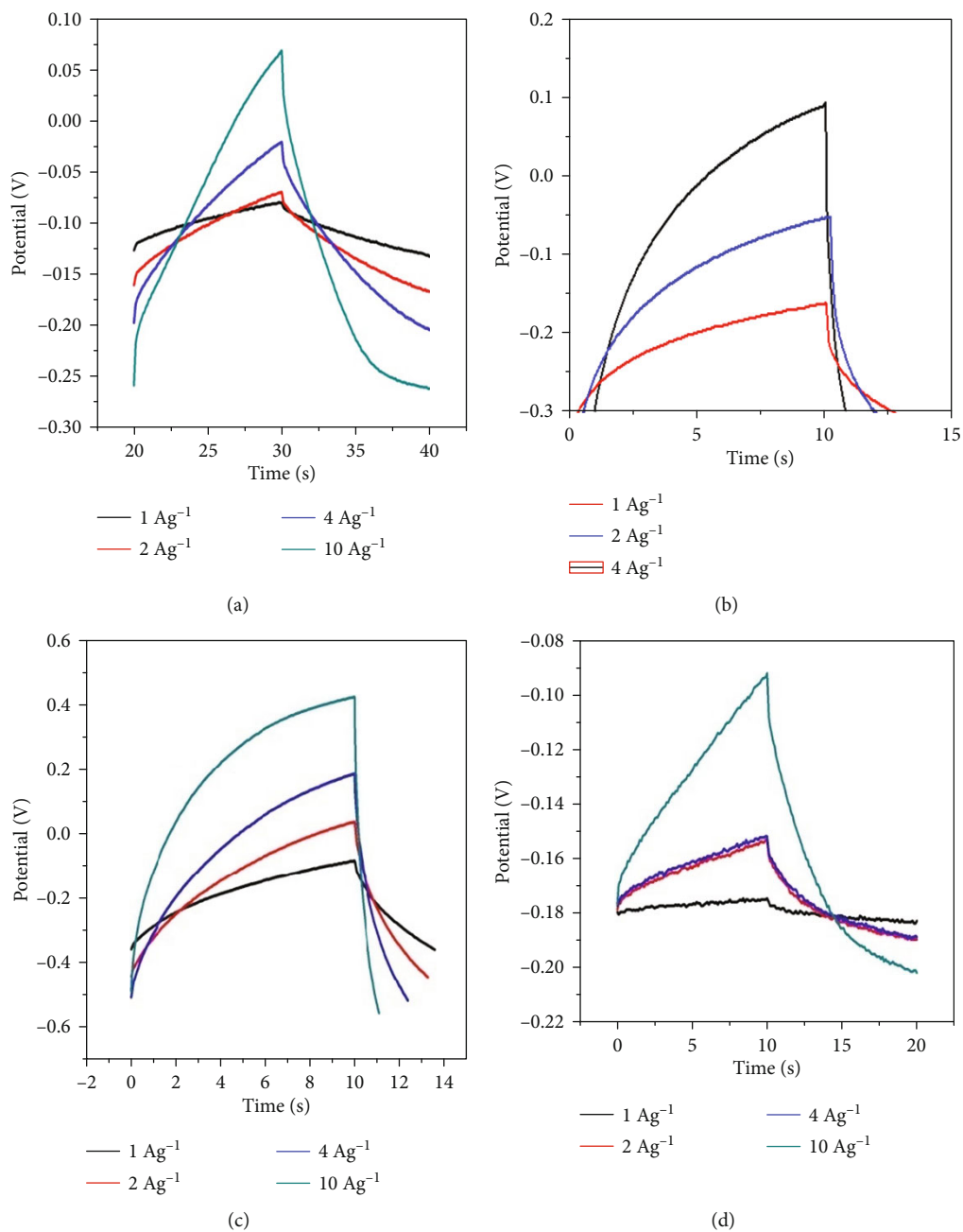
Figure 6: GCD curve of (a) GO, (b) GO/PPY, (c) GO/PPy/ACZJ, and (d) GO/PPy/ACPD.

Table 1: Specific capacitance of prepared samples.

Samples	1 A g^{-1}	2 A g^{-1}	4 A g^{-1}	10 A g^{-1}
GO	144.3	102	53.2	32.8
GO/MnO$_2$	87.3	45.3	25.5	14.4
GO/PPy	47.93	24.38	12.43	0.11
ACZJ	264.75	102	25.25	25.5
ACPD	434.78	237.55	105.9	50.5
GO/PPy/ACZJ	13.1	6.85	3.42	1.14
GO/PPy/ACPD	1217.1	456.67	270.44	90.88

Table 2: Energy and power density of prepared samples.

Samples	Energy density, Wh g^{-1}	Power density, W g^{-1}
GO	0.47	160
GO/MnO$_2$	0.98	350
GO/PPy	1.11	402.02
ACZJ	0.57	200
ACPD	0.28	100
GO/PPy/ACZJ	0.15	489
GO/PPy/ACPD	0.15	55.02
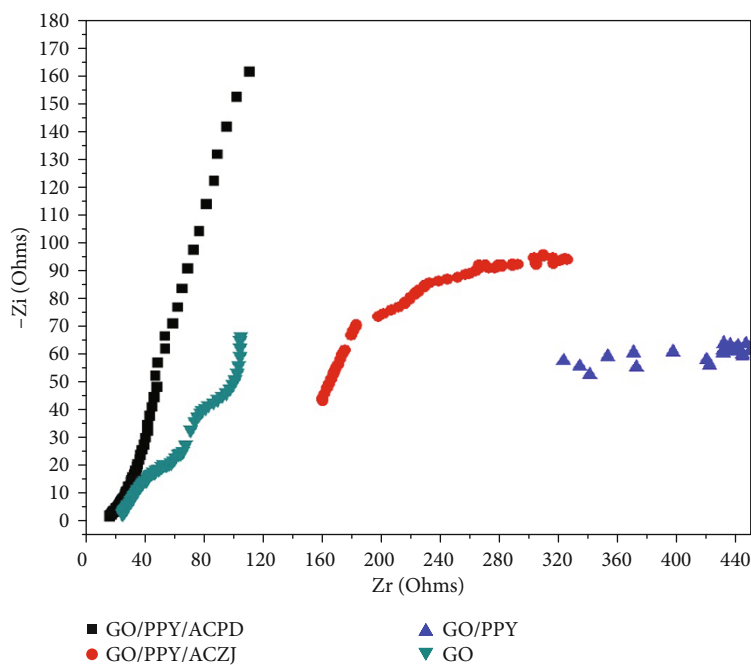
Figure 7: EIS curve of the prepared samples.

prepared samples were coated on a graphite lead of 2-mm thickness using a puncture sealant as binding material. The electrochemical analysis was performed in an electrochemical workstation.

3. Result and Discussion

Figure 1shows the XRD of GO, GO/PPy, GO/PPy/ACZJ, and GO/PPy/ACPD composite. Weak and broad diffraction peak is observed at 20° and 19°, for GO/PPY/ACZJ and GO/PPY/ACPD, respectively, with d-spacing 0.467 and 0.492 nm.

Also some of the weak peak is at 27° for GO/PPY/ACZJ composite. Similarly, weak peak is observed at 36° for GO/PPY/ACPD composite. Here, increased d-spacing is observed at GO/PPY/ACPD, due to the introduction of O_2 containing groups than GO/PPY/ACZJ composite.

The FTIR spectra of GO, GO/PPy, GO/PPy/ACZJ, and GO/PPy/ACPD is shown in Figure 2. From this, the oxygen functional groups of GO are identified from the peaks 702.09 and 2978.08 cm^{-1}, corresponding to C=C bending and C-H stretching, respectively. The peaks of GO/PPy at 786.96, 1165, 1535, 1734, and 2978 cm^{-1} correspond to C=C bending, C-N stretching wagging vibration, C=C stretching, C=O band stretching, and C-H stretching, respectively.

For the ternary composite (GO/PPy/ACZJ), the peaks observed at 786.96, 1214, 1486, and 2978.09 cm^{-1} corresponds to C=C bending, C-N stretching wagging vibration, C=C stretching, and C-H stretching, respectively. Finally, the peaks observed at 786.96, 1265, 1502, and 2978 cm^{-1} correspond to C=C bending, C-N stretching wagging vibration, C=C stretching, and C-H stretching, respectively.

The SEM images of GO is shown in Figure 3(a) at 5 k × magnifications at a voltage of about 20 kV. From the image, it is observed that GO has stacked layers with porosity. Sim-

ilarly, sphere-like morphology is observed for the GO/PPy composite shown in Figure 3(b). From Figure 3(c), sheet-like morphology is observed for GO/PPy/ACZJ with limited pores. Figure 3(d) shows more pores than ternary composite made from graphene oxide, polypyrrole, and activated carbon obtained from the seeds of *Ziziphus jujuba*.

From the EDX analysis shown in Figure 4, higher amount of carbon content is observed for the binary composite. Similarly, it is observed for the ternary composite. The performance of the electrode was analyzed by cyclic voltammetry, galvanostatic charge and discharge measurements, and electrochemical impedance spectroscopy using OrigaLys electrochemical workstation, and the results are shown below.

CV analysis was carried out to investigate the reduction and oxidation processes of the materials. The CV curves of the electrodes are collected in the range of 0 to 1 V. The electrochemical activity of the GO/PPy/AC composites such as GO/PPy/ACZJ and GO/PPy/ACPD electrodes is shown in Figure 5. It is observed that GO/PPy/ACPD composite illustrates the better nature than GO/PPy/ACZJ. Similarly, GO/PPy/ACPD showed better area. The increased area of GO/PPy/ACPD helps in improving the specific capacitance.

To further confirm the CV analysis, GCD measurements for the GO, GO/PPy, GO/PPy/ACZJ, and GO/PPy/ACPD composites were done for different current density. Figure 6 shows the GCD curves of GO, GO/PPy, GO/PPy/ACZJ, and GO/PPy/ACPD electrodes. Specific capacitance values for all the samples are listed in Table 1. It was observed from the quasi triangular curve that the GO/PPy/ACPD composite owns capacitive properties and electrochemical reversibility in support of the progress of a supercapacitor. When compared to GO alone, the GO/PPy composite exhibited lowest specific capacitance. This may be due to the sacrificial

template, and the presence of PPy blocks the pores presented in GO. Similarly, ACZJ alone exhibited 264.75 F g^{-1} at 1 Ag^{-1}. But, when it is composited, the GO/PPy has been changed as GO/PPy/ACZJ electrode with specific capacitence of 13.1 F g^{-1}. Finally, GO/PPY/ACPD exhibited the specific capacitance of 1217.1 F g^{-1} at 1 A g^{-1}. Similarly, due to the instability of PPy, the specific capacitance reached to the lowest level at 10 A g^{-1}. Energy and power density of the samples are listed in Table 2. From the GCD measurements, high power density is observed for GO/PPy/ACZJ.

For GO, at 0.46 Wh g^{-1} energy density, the power density of 160 W g^{-1} is obtained. In supercapacitor-based energy storage, the researchers were tried to improve the power density. In this research, the highest power density is observed. It may be a breakthrough for the further research. From the GCD measurements, high power density is observed for GO/PPy/ACZJ. EIS analysis of GO, GO/PPy, GO/PPy/ACZJ, and GO/PPy/ACPD electrodes was done in the frequency of 100 kHz to 0.01 Hz as shown in Figure 7. In OrigaLys electrochemical workstation, the supported frequency is 100 kHz (high frequency) to 0.01 Hz (low frequency).

The semicircle at high-frequency and a straight line in the low-frequency indicates an electrical conductivity and ions diffusion behavior. From the Nyquist plot, it is observed that the series resistance (R_s) exhibited 30 Ω, for the sample GO. Similarly, the charge-transfer resistance (R_{ct}) of 16 Ω was obtained for GO. But GO/PPy samples exhibited very higher series and charge transfer resistance due to the addition of polypyrrole.

At the same time, series resistance of GO/PPy/ACZJ was smaller than GO/PPy binary composite. Almost Warburg resistance is observed for both the ternary composites. Compared to GO/PPy/ACZJ, the GO/PPy/ACPD composite electrode demonstrated lower resistances which led to higher conductivity. From the Figure 7, R_s and R_{ct} of GO/PPy/ACZJ were computed as 160 Ω and 15 Ω, respectively. In the same way, R_s and R_{ct} of GO/PPy/ACPD electrode were measured as 20 Ω and 30 Ω, respectively. These resistances contributed higher specific capacitance as described in GCD measurements.

4. Conclusion

In this research, the ternary composites of graphene oxide, activated carbon, and polypyrrole were synthesized through modified hummers' method, sacrificial template polymerization method, and hydrothermal method. Because of the larger surface area, greater conductivity and also ability to optimization of activated carbon leads to enhanced electrochemical supercapacitor. Initially AC was derived from biomaterials such as seeds of *Ziziphus jujuba* and shells of *Prunus dulcis*. The electrochemical performances of GO, GO/PPy, GO/PPy/ACZJ, and GO/PPy/ACPD electrodes were evaluated using 6 M KOH. From the GCD curves, the GO/PPy/ACPD showed an enhanced electrochemical performance and high stability. In GO/PPy/ACZJ electrode, the specific capacitances are 13.1, 6.85, 3.42 F g^{-1}, and 1.14 F g^{-1} at 1, 2, 4, and 10 A g^{-1}, respectively. Surprisingly, the GO/PPy/ACPD electrode exhibited the specific capaci-

tance of 1217.1, 456.67, 270.44, and 90.88 F g^{-1} at the same current density. GO/PPy/ACPD composite revealed the highest specific capacitance of 1217.1 F g^{-1} at 1 A g^{-1} in 6 M KOH. High electrochemical performances were attributed for GO/PPy/ACPD. Overall, GO/PPy/ACPD composite exhibited the highest specific capacitance, and this ternary composite may fill the potential drawbacks of existing flexible supercapacitor.

Data Availability

All the data are used for this manuscript.

Conflicts of Interest

The authors declare that they have no conflicts of interest.

Acknowledgments

References

[1] S. K. Kandasamy and K. Kandasamy, "Recent advances in electrochemical performances of graphene composite (graphene-polyaniline/polypyrrole/activated carbon/carbon nanotube) electrode materials for supercapacitor: a review," *Journal of Inorganic and Organometallic Polymers*, vol. 28, no. 3, pp. 559–584, 2018.

[2] M. Devendran, S. K. Kandasamy, S. Palanisamy et al., "Preparation of chemically modified porous carbon networks derived from Citrus sinensis flavedos as electrode material for supercapacitor," *International Journal of Electrochemical Science*, vol. 15, pp. 4379–4387, 2020.

[3] K. Senthil Kumar, A. Chandrasekaran, L. Vadivel, M. Ganapathi, N. K. Nattudurai, and K. Kandasamy, "Synthesis of Chemically Modified Activated Carbon for Supercapacitor Electrode Derived from Fibers of Musa paradisiacal," *International Journal of Emerging Technologies*, vol. 11, pp. 565–569, 2020.

[4] K. Senthil Kumar, A. Chandrasekaran, and K. Kannan, "Effects of microwave annealing of graphene and its impact on structural, electrochemical performance for energy storage," in *2018 International Conference on Intelligent Computing and Communication for Smart World (I2C2SW)*, vol. 241, Erode, India, December 2018.

[5] D. Sivalingam, H. Elangovan, M. Subramanian, S. K. Kandasamy, and M. Govindasamy, "Synthesis and characterization of PANI/ferric chloride composite for fabrication of electrodes in supercapacitor," *Advances in Materials Research*, vol. 768, pp. 334–337, 2013.

[6] S. Yadav and A. Devi, "Recent advancements of metal oxides/ Nitrogen-doped graphene nanocomposites for supercapacitor electrode materials," *Journal of Energy Storage*, vol. 30, article 101486, 2020.

[7] M. Gandara and E. S. Goncalves, "Polyaniline supercapacitor electrode and carbon fiber graphene oxide: electroactive properties at the charging limit," *Electrochimca Acta*, vol. 345, article 136197, 2020.

[8] S. K. Kandasamy and K. Kandasamy, "Structural and electrochemical analysis of microwave-assisted synthesis of graphene/polypyrrole nanocomposite for supercapacitor," *International Journal of Electrochemical Science*, vol. 14, no. 5, pp. 4718–4729, 2019.

[9] U. Male and J. K. R. Modigunta, "Design and synthesis of polyaniline-grafted reduced graphene oxide via azobenzene pendants for high-performance supercapacitors," *Polymer*, vol. 110, pp. 242–249, 2017.

[10] S. K. Kandasamy and K. Kandasamy, "Graphene–Polyaniline Nanocomposite Treated with Microwave as a New Supercapacitor Electrode and its Structural, Electrochemical Properties Graphene–Polyaniline Nanocomposite Treated with Microwave as a New Supercapacitor Electrode and its Structural, Electrochemical Properties," *Journal of New Materials for Electrochemical Systems*, vol. 22, pp. 125–131, 2019.

[11] Y. Guo, L. Zhang, Y. Liu, and S. Guo, "Almond Shell-Derived Carbons under Low-Temperature Activation with Ultra-High Surface Area and Superior Performance for Supercapacitors," *Chemistry Select*, vol. 4, no. 43, pp. 12472–12478, 2019.

[12] Y. Li, K. Zheng, S. A. Ali Shah et al., "Winter-jujube-derived carbon with self-doped heteroatoms and a hierarchically porous structure for high-performance supercapacitors," *RSC Advances*, vol. 7, no. 69, pp. 43356–43365, 2017.

[13] K. Sun, S. Yu, Z. Hu et al., "Oxygen-containing hierarchically porous carbon materials derived from wild jujube pit for high-performance supercapacitor," *Electrochimica Acta*, vol. 231, pp. 417–428, 2017.

[14] V. Yang, S. R. Arumugam, J. Pan, T. Rajeshkumar, Y. Sun, and X. Liu, "Metal Oxide Nanoparticles as Biomedical Materials," *The Journal of Colloid and Interface Science*, vol. 5, no. 2, article 27, 2020.

[15] A. G. Theophil, D. Renuka, R. Ramesh et al., "Green synthesis of ZnO nanoparticle using _Prunus dulcis_ (Almond Gum) for antimicrobial and supercapacitor applications," *Surface Interface*, vol. 17, article 100376, 2019.

[16] C. D. Jiménez, F. Heras, M. A. Gilarranz, and P. E. Raymundo, "Activation of waste tire char by cyclic liquid-phase oxidation," *Carbon*, vol. 127, pp. 157–162, 2014.

[17] O. E. Eleri, K. U. Azuatalam, M. W. Minde et al., "Towards high-energy-density supercapacitors via less-defects activated carbon from sawdust," *Electrochimica Acta*, vol. 362, article 137152, 2020.

[18] M. Vinayagam, B. R. Suresh, A. Sivasamy, and D. A. Ferreira, "Biomass-derived porous activated carbon from Syzygium cumini fruit shells and Chrysopogon zizanioides roots for high-energy density symmetric supercapacitors," *Biomass and Bioenergy*, vol. 143, article 105838, 2020.

[19] R. M. Usha, K. Nanaji, T. N. Rao, and A. S. Deshpande, "Corn husk derived activated carbon with enhanced electrochemical performance for high-voltage supercapacitors," *Journal of Power Sources*, vol. 471, article 228387, 2020.

[20] S. J. Rajasekaran and V. Raghavan, "Facile synthesis of activated carbon derived from *Eucalyptus globulus* seed as efficient electrode material for supercapacitors," *Diamond and Related Materials*, vol. 109, article 108038, 2020.

[21] H. N. Van, P. A. Dat, H. N. Van, T. N. Le, N. C. Minh, and T. N. Van, "Rapid and efficient synthesis of high-porous reduced graphene oxide/NiCo2S4 nanocomposites for supercapacitor application," *Diamond and Related Materials*, vol. 106, article 107850, 2020.

[22] Z. Wang, L. Jiang, Y. Wei, and C. Zong, "In-situ polymerization to prepare reduced graphene oxide/polyaniline composites for high performance supercapacitors," *Journal of Energy Storage*, vol. 32, article 101742, 2020.

[23] A. Rose, P. K. Guru, T. Sakthivel, V. Gunasekaran, T. Maiyalagan, and T. Vijayakumar, "Electrochemical analysis of graphene oxide/polyaniline/polyvinyl alcohol composite nanofibers for supercapacitor applications," *Applied Surface Science*, vol. 449, pp. 551–557, 2018.

[24] H. Wang, Q. Hao, X. Yang, L. Lu, and X. Wang, "Graphene oxide doped polyaniline for supercapacitors," *Electrochemistry Communications*, vol. 11, pp. 1158–1161, 2009.

[25] P. Asen, S. Shahrokhian, and A. I. Zad, "Transition metal ions-doped polyaniline/graphene oxide nanostructure as high performance electrode for supercapacitor applications," *Journal of Solid State Electrochemistry*, vol. 22, no. 4, pp. 983–996, 2018.

[26] N. A. Kumar, J. C. Hyun, R. S. Yeon, W. C. Dong, D. Liming, and B. B. Jong, "Tensile strain switched ferromagnetism in layered NbS2 and NbSe2," *ACS Nano*, vol. 6, no. 11, pp. 9727–9736, 2012.

[27] K. Senthil Kumar, A. Chandrasekaran, A. S. Sajitha et al., "Chemically Treated Activated Carbon for Supercapacitor Electrode Derived from Starch of Solanum Tuberosum," *Journal of New Materials for Electrochemical Systems*, vol. 24, pp. 78–83, 2021.

[28] S. B. Vinay, K. Pandiyaraj, S. Ganesan et al., "Low cost, catalyst free, high performance supercapacitors based on porous nano carbon derived from agriculture waste," *Journal of Energy Storage*, vol. 32, article 101829, 2020.

[29] R. Bhimanaboina, N. S. Goli, S. Chandra, and S. Y. Jae, "Waste tissue papers templated highly porous Mn3O4 hollow microtubes prepared via biomorphic method for pseudocapacitor applications," *Journal of Alloys and Compounds*, vol. 772, pp. 925–932, 2019.

[30] L. Yuhao, Q. Xiaoxiao, H. Guangxu et al., "3-Dimensional porous carbon with high nitrogen content obtained from longan shell and its excellent performance for aqueous and all-solid-state supercapacitors," *Journal of Nanomaterials*, vol. 10, no. 4, Article ID 808, 2020.

[31] Z. Yan Lei and T. Zhi Shu, "Porous carbon derived from herbal plant waste for supercapacitor electrodes with ultrahigh specific capacitance and excellent energy density," *Waste Management*, vol. 106, pp. 250–260, 2020.

[32] J. R. Sofia and R. Vimala, "Facile synthesis of activated carbon derived from *Eucalyptus globulus* seed as efficient electrode material for supercapacitors," *Diamond and Related Materials*, vol. 109, article 108038, 2020.

[33] L. Kenny, S. Luba, N. F. Shaikh, C. H. Van, and G. G. J. Vincent, "Aerogel from fruit biowaste produces ultracapacitors with high energy density and stability," *Journal of Energy Storage*, vol. 27, article 101152, 2020.

[34] L. Dawei, C. Mingyan, L. Yucheng et al., "Preparation and characterization of high value-added activated carbon derived from biowaste walnut shell by KOH activation for supercapacitor electrode," *Journal of Materials Science: Materials in Electronics*, vol. 31, no. 21, pp. 18541–18553, 2020.

[35] N. V. T. Le PA, S. K. Sahoo, T. Y. Tseng, and K. H. Wei, "Porous carbon materials derived from areca palm leaves for high performance symmetrical solid-state supercapacitors," *Journal of Materials Science*, vol. 55, no. 24, pp. 10751–10764, 2020.

[36] V. Murugan, S. B. Rajendran, S. Arumugam, and L. F. B. Ana, "Biomass-derived porous activated carbon from *Syzygium*

cumini fruit shells and *Chrysopogon zizanioides* roots for high-energy density symmetric supercapacitors," *Biomass and Bioenergy*, vol. 143, article 105838, 2020.

[37] M. S. Karnan, B. Suresh, K. Subramani, K. Raja, V. Sannasi, and M. Sathish, "Electrochemical performance of *Thespesia populnea* seeds derived activated carbon - supercapacitor and its improved specific energy in redox additive electrolytes," *Journal of Energy Storage*, vol. 32, article 101939, 2020.

[38] S. A. E. Khodary, I. S. Yahia, H. Y. Zahran, and M. Ibrahim, "Preparation of polypyrrole-decorated MnO2/reduced graphene oxide in the presence of multi-walled carbon nanotubes composite for high performance asymmetric supercapacitors," *Physica B: Condensed Matter*, vol. 556, pp. 66–74, 2018.

[39] C. Arumugam, K. K. Senthil, R. Sabitha, M. Sangavi, and P. T. Ruthra, "Hierarchical structure of graphene oxide/MnO2 electrodes for supercapacitor," *AIP Conference Proceedings*, vol. 2387, no. 1, article 090004, 2021.

[40] C. Arumugam, K. K. Senthil, G. Keerthika, S. Kirubasri, and P. E. Krishna, "Hierarchical structure of graphene oxide/polyaniline composite flexible supercapacitor," *AIP Conference Proceedings*, vol. 2387, no. 1, article 090003, 2021.

[41] S. Nirmaladevi, R. Boopathiraja, S. K. Kandasamy, S. Sathishkumar, and M. Parthibavarman, "Wood based biochar supported MnO2 nanorods for high energy asymmetric supercapacitor applications," *Surfaces and Interfaces*, vol. 27, article 101548, 2021.

[42] P. Shanmugam, S. K. Kandasamy, T. Sathesh et al., "Synthesis of activated carbon from black liquor for the application of supercapacitor," *Journal of Materials Science: Materials in Electronics*, vol. 32, no. 20, pp. 25175–25187, 2021.

[43] S. K. Kandasamy, A. Chandrasekaran, V. Logupriya, K. Saravanakumar, and K. Deepa, "Fabrication of ZnO–Carbonized cotton yarn derived hierarchical porous active carbon flexible electrodes," *AIP Conference Proceedings*, vol. 2387, no. 1, article 090005, 2021.

[44] S. K. Kandasamy, N. S. Kavitha, K. Hemalatha et al., "Microwave-assisted graphene-based conducting polymer materials for supercapacitors," in *Handbook of Supercapacitor Materials: Synthesis, Characterization, and Applications*, vol. 299, Wiley, 2021.